

# An examination of the role of plasma treatment for lean $\text{NO}_x$ reduction over sodium zeolite Y and gamma alumina

## Part 1. Plasma assisted $\text{NO}_x$ reduction over NaY and $\text{Al}_2\text{O}_3$

S. Yoon, A.G. Panov, R.G. Tonkyn, A.C. Ebeling, S.E. Barlow, M.L. Balmer\*

*Pacific Northwest National Laboratory, Richland, WA, USA*

### Abstract

The role of plasma processing on  $\text{NO}_x$  reduction over  $\gamma$ -alumina and a basic zeolite, NaY was examined. During the plasma treatment NO is oxidized to  $\text{NO}_2$  and propylene is partially oxidized to CO,  $\text{CO}_2$ , acetaldehyde, and formaldehyde. With plasma treatment, NO as the  $\text{NO}_x$  gas, and a NaY catalyst, the maximum  $\text{NO}_x$  conversion was 70% between 180 and 230 °C. The activity decreased at higher and lower temperatures.

As high as 80%  $\text{NO}_x$  removal over gamma alumina was measured by a chemiluminescent  $\text{NO}_x$  meter with plasma treatment and NO as the  $\text{NO}_x$  gas.

For both catalysts a simultaneous decrease in  $\text{NO}_x$  and aldehydes concentrations was observed, which suggests that aldehyde may be important components for  $\text{NO}_x$  reduction in plasma-treated exhaust. © 2002 Elsevier Science B.V. All rights reserved.

**Keywords:** Chemiluminescent; Compression ignition; Zeolite

### 1. Introduction

The US environmental protection agency (EPA) has been regulating volatile organic compounds (VOCs), nitrogen oxides ( $\text{NO}_x$ ), and carbon monoxide (CO) from automobile sources since the 1970s. On-road vehicles today are approximately 95% cleaner per mile compared to a new vehicle sold in the 1960s [1]. However, as Americans continue to purchase more cars per household and drive more miles per year, the overall national pollution levels continue to rise. Lean burn gasoline and diesel compression ignition (CI) engines provide significant fuel economy benefits compared to common gasoline engines operating under

stoichiometric air–fuel conditions. However, current three-way catalyst exhaust after-treatment technologies are ineffective in reducing  $\text{NO}_x$  under lean burn exhaust conditions (Table 1).

More stringent environmental regulations have resulted in considerable research into ways of reducing harmful manmade exhaust emissions. The ongoing research is leading to innovative applications of new technologies to resolve these environmental issues.

A need for an effective after treatment process capable of reducing  $\text{NO}_x$  in an oxygen rich environment has produced a large interest in plasma assisted catalytic reduction. [2–8] There have been a number of reports that show that a plasma combined with a catalyst can reduce from 60 to 80%  $\text{NO}_x$  in simulated diesel and lean burn exhaust. In particular, gamma alumina and zeolitic catalysts have shown high activity when preceded by a plasma [5,6].

\* Corresponding author. Present address: Caterpillar Inc., Technology Center E/854, P.O. Box 1875, Peoria, IL 61656-1875, USA. Tel.: +1-309-578-4468; fax: +1-309-578-2953.  
E-mail address: balmer-millar\_lou@cat.com (M.L. Balmer).

Table 1

Average engine exhaust concentrations for spark ignition (SI) and diesel CI engines for the EPA's US Federal Test Procedure (FTP) cycle

	Typical concentration of exhaust gas <sup>a</sup> (automobile exhaust)	Lean burn concentration of exhaust gas <sup>a</sup>
Hydrocarbons (ppm)	750 <sup>b</sup>	700 <sup>b</sup>
NO <sub>x</sub> (ppm)	1050	260
CO	0.68%	400 ppm
H <sub>2</sub>	0.23%	130 ppm
CO <sub>2</sub> (%)	13.50	7
O <sub>2</sub> (%)	0.51	8
H <sub>2</sub> O (%)	12.50	7

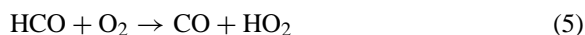
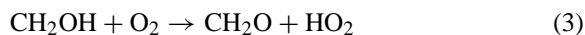
<sup>a</sup> Concentrations are based on volume.

<sup>b</sup> Based on C<sub>8</sub>.

While the chemistry in the plasma can be quite complex, it is widely accepted that in the presence of hydrocarbons in a lean burn effluent, plasma processing will oxidize NO to NO<sub>2</sub>. Using propylene as the representative hydrocarbon, Penetrante et al. [7,8] conclude that NO oxidation is primarily due to the following reactions:



where *R* is a hydrocarbon radical. The HO<sub>2</sub> radicals are produced from reactions involving hydrocarbon intermediates of propylene oxidation [7]. The hydrocarbons are oxidized in the plasma, however the oxidation does not proceed completely to CO<sub>2</sub> and H<sub>2</sub>O. Penetrante proposes the following reactions involving hydrocarbon intermediates to form HO<sub>2</sub> radicals [7]:



The purpose of this study is to examine the significance of plasma processing on NO<sub>x</sub> reduction over γ-alumina and a basic zeolite NaY.

## 2. Experimental

### 2.1. Experimental plasma-catalyst apparatus

The experimental plasma-catalyst apparatus was a two-stage configuration as shown in Fig. 1. The reactor system consists of a double dielectric-barrier discharge reactor followed by a quartz catalytic reactor tube. The catalytic reactor is capable of testing powders, pellets, and coated monoliths at various temperatures.

The plasma and catalyst reactors were heated separately by two cylindrical ceramic fiber heaters (WATLOW). The plasma reactor temperature was maintained at 110 °C for all tests to prevent water condensation and the catalyst reactor temperature was controlled to the desired temperature.

Mass flow controllers were used to control and regulate the influent gases (MKS Type 1179A and Tylan Model FC-260). A fraction of the flow was diverted to a water bubbler to adjust the relative humidity of the gas stream. A humidity transmitter (Vaisala HMP 235) in the gas manifold was used to measure and regulate the water concentration.

After the gas constituents were combined and mixed in the gas manifold, a three-way valve allowed the gas stream either to enter the plasma reactor or bypass the plasma and catalyst reactors entirely for influent gas calibration (Fig. 1). A valve between the plasma and catalyst reactors allowed the gas leaving the plasma region to bypass the catalyst. This feature enables the analysis of the products formed in the plasma alone.

The gas hourly space velocities (GHSV) which were determined from the standard flow rate of the gas divided by the catalyst bed volume, was 12,000 h<sup>-1</sup> in the catalyst reactor. The typical GHSV within the plasma reactor was 30,000–60,000 h<sup>-1</sup>. The effective operation of the plasma reactor is relatively insensitive to space velocity.

The effluent gas was analyzed by a chemiluminescent NO<sub>x</sub> analyzer (CLNA) (Beckman Model 951) and a Fourier transform infrared (FTIR) spectrometer (Nicolet Magna 560) equipped with a heated 2 m gas cell. For each FTIR spectrum, 50 scans were collected at 0.5 cm<sup>-1</sup> resolution. Measured absorbencies were converted to concentrations from calibration plots.

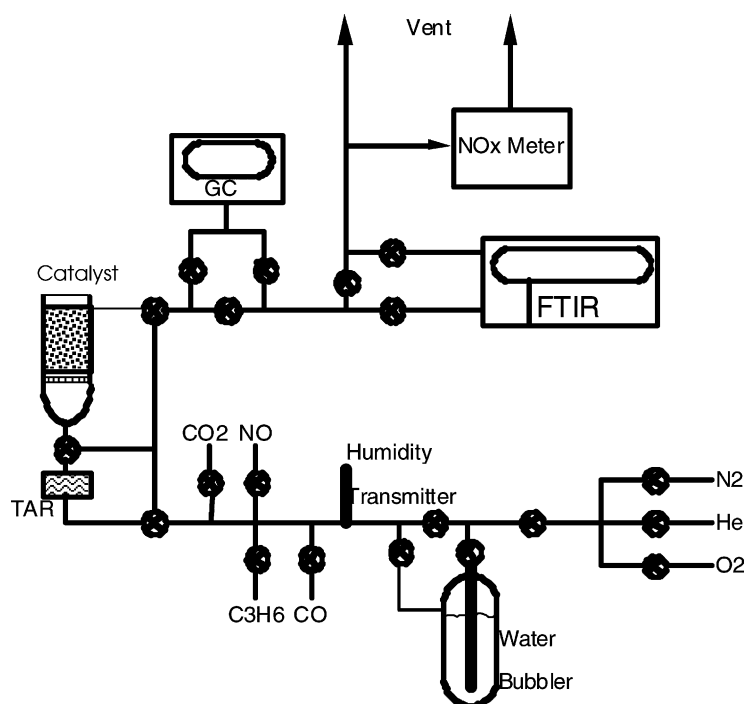


Fig. 1. Schematic layout of two-stage plasma-catalyst experimental apparatus: TAR; GC—micro gas chromatograph; FTIR spectrometer; NO<sub>x</sub> meter—chemiluminescent NO<sub>x</sub> analyzer.

## 2.2. Plasma reactor and power measurement

The use of dielectric-barrier discharge processing is a mature technology, and is routinely used for water purification and bleaching applications [9]. The silent discharge plasma reactor used in this study consists of a bed of stainless steel rod electrodes encased in closed-ended alumina rods acting as a dielectric barrier. This particular design is designated the tube-array plasma reactor (TAR). A cross-sectional view of the TAR is shown in Fig. 2. This design was selected to utilize the electrical efficiency of cylindrical high voltage and ground electrodes with small diameters and to minimize the gap distance between the electrodes.

For typical catalytic systems, control and measurement of the gas flow and analysis of the composition is essential. However, for plasma-catalysis systems, the power measurement is also an important aspect. The power measurement circuit used was directly adapted from Rosenthal [10] and described in detail by Tonkyn et al. [11]. The energy dissipated per cycle is

given by

$$\begin{aligned}
 E &= \int_0^\tau P(t) dt = \int_0^\tau V(t)i(t) dt \\
 &= \int_0^\tau V(t) dq(t) = C \oint_\tau V(t) dV_C(t)
 \end{aligned} \quad (7)$$

Here  $\tau$  is the period of the driving wave form,  $P$  the delivered power,  $V$  the input high voltage,  $i$  the current

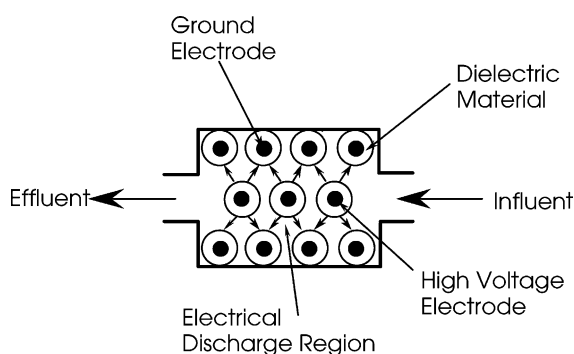


Fig. 2. Schematic of cross-sectional view of the TAR.

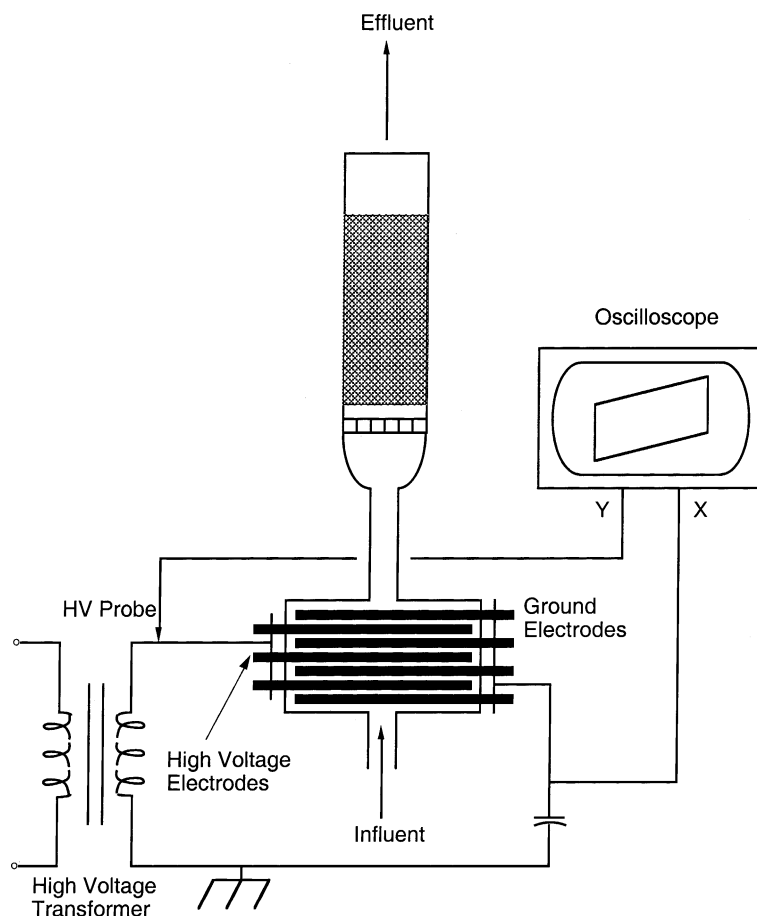


Fig. 3. Simplified drawing of the power delivery set-up and the power measurement circuit for the TAR; HV probe: high voltage probe.

flow,  $q$  the charge transported across the reactor,  $C$  the capacitance of the series capacitor, and  $V_C$  the voltage across that capacitor. This integral is experimentally evaluated by numerical analysis of the area inside a trace formed by plotting the input voltage versus the capacitive voltage on an oscilloscope. The result yields the energy deposited in the reactor per cycle. A simplified drawing of the power delivery to the TAR and the power measurement circuit is shown in Fig. 3.

### 3. Results and discussion

#### 3.1. Chemistry in the plasma

In order to define the role of the plasma on NO chemistry in a simulated lean mix, a CLNA was used

to measure the concentrations of NO and NO<sub>2</sub> as a function of plasma energy density. The lean mix contained 200 ppm NO in a N<sub>2</sub> bath gas with 575 ppm propylene, 125 ppm propane, 400 ppm CO, 130 ppm H<sub>2</sub>, 0.9% argon, 7% CO<sub>2</sub>, 8% O<sub>2</sub>, and 2% water. The NO and NO<sub>2</sub> concentrations as a function of electrical energy density are shown in Fig. 4. The temperature of the plasma reactor was kept at 100 °C. As the energy density (Joules/liter) is increased, an exponential decrease in the concentration of NO is observed. Correspondingly, an exponential increase in the formation of NO<sub>2</sub> is observed with increasing energy density. This observation agrees well with the published reports [7,12,13].

It can be seen that with plasma treatment alone, the total NO<sub>x</sub> concentration appears to remain relatively

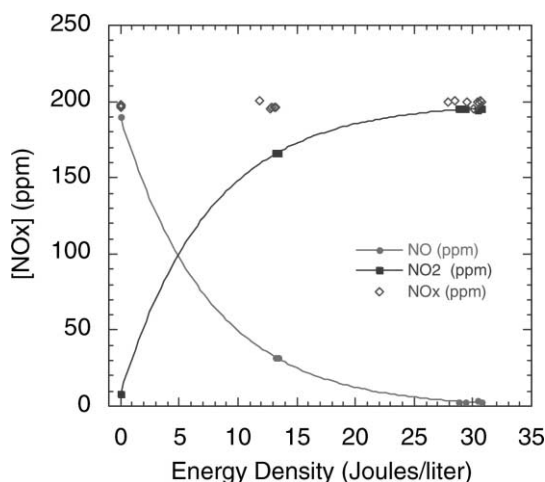


Fig. 4. The  $\text{NO}_x$  concentration as a function of energy density. The concentrations of the constituents in the  $\text{N}_2$  bath gas were 200 ppm NO, 575 ppm propylene, 125 ppm propane, 400 ppm CO, 130 ppm  $\text{H}_2$ , 0.9% argon, 7%  $\text{CO}_2$ , 8%  $\text{O}_2$ , and 2% water.

constant (Fig. 4). However, a 5–15% overall decrease in  $\text{NO}_x$  concentration is also observed with plasma only. This “missing”  $\text{NO}_x$  is converted to NO when 5 ml of 3%  $\text{Pt}/\text{Al}_2\text{O}_3$  catalyst At  $300^\circ\text{C}$  (GHSV = 24,000) is placed downstream of the plasma. There has been speculation that treatment of lean  $\text{NO}_x$  with plasma alone can reduce  $\text{NO}_x$  to  $\text{N}_2$ . However, since the missing nitrogen atoms can be completely recovered as  $\text{NO}_x$  with an oxidation catalyst, it can be concluded that  $\text{NO}_x$  reduction to  $\text{N}_2$  is not occurring within the plasma.

In addition to oxidation of NO to  $\text{NO}_2$ , FTIR and mass spectrometer analysis of the effluent gas show that the hydrocarbon is oxidized by the plasma treatment. The oxidation of the hydrocarbon is incomplete over the energy range necessary to completely oxidize NO to  $\text{NO}_2$  resulting in a mix of aldehydes, CO, and  $\text{CO}_2$  during plasma treatment.

For typical synthetic exhaust mixture, at the plasma reactor temperature  $100^\circ\text{C}$  and  $\text{C}_3\text{H}_6$  concentration at input 700 ppm, 36% of propylene is converted to different oxidation products. The oxidation products distribution was determined with FTIR. Twenty percent of converted propylene formed formaldehyde, 50% acetaldehyde, 20% CO and  $\text{CO}_2$  and the rest was converted to organic nitrates.

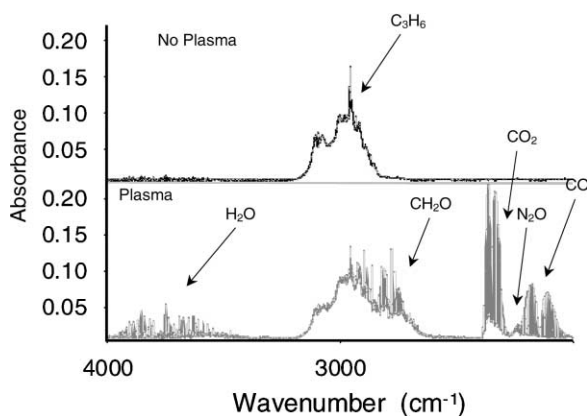


Fig. 5. FTIR spectrum of a simplified lean burn exhaust with plasma treatment and without plasma treatment. The exhaust concentration consisted of 200 ppm NO, 700 ppm  $\text{C}_3\text{H}_6$ , and 8%  $\text{O}_2$  in helium.

Figs. 5 and 6 compare the FTIR spectra of a simplified simulated lean burn exhaust mix with and without plasma processing. The typical lean burn exhaust was simplified to eliminate all unreactive constituents in the exhaust and to allow easier analysis of the spectra. The concentrations of the constituents were 200 ppm NO, 700 ppm propylene, and 8%  $\text{O}_2$  in a  $\text{N}_2$  bath. The power density for these experiments was about 40 J/l. At this energy level, as seen from Fig. 4, nearly

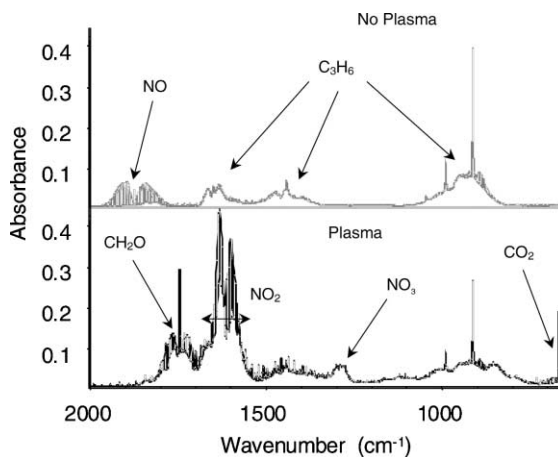


Fig. 6. FTIR spectrum of a simplified lean burn exhaust with plasma treatment and without plasma treatment. The exhaust concentration consisted of 200 ppm NO, 700 ppm  $\text{C}_3\text{H}_6$ , and 8%  $\text{O}_2$  in helium.

complete NO to NO<sub>2</sub> conversion is expected. Penetrante et al. [14] and Balmer et al. [16] have reported that neither CO nor CO<sub>2</sub> contribute to the observed oxidation chemistry of the plasma [15]. This will be supported further in the nitrogen balance experimental data to follow. Experiments conducted with and without water in the gas mix show by FTIR analysis that the observed species formed in the plasma do not change. Therefore, the water was also removed from the gas mix due to the overwhelming number of features in the FTIR spectrum associated with water.

In Fig. 5, the FTIR spectrum of the simplified lean burn exhaust is shown with and without plasma processing for the wave number region between 4000 and 2000 cm<sup>-1</sup>. Without plasma, the distinct features representative of propylene can be seen at the C–H stretching region (~3000 cm<sup>-1</sup>). No other features are present in this spectral region without plasma treatment of the exhaust. With plasma processing, the features indicative of H<sub>2</sub>O, CO<sub>2</sub>, N<sub>2</sub>O and CO are easily detected in the spectra (Fig. 5). Also, the distinguishable C–H stretch peaks associated with formaldehyde (CH<sub>2</sub>O) are observed at a wave number region near 2780 cm<sup>-1</sup>. In this region, the C–H stretch associated with larger aldehydes can also be observed. However, due to the wide band widths associated with these molecules, verification is difficult. According to the FTIR data which shows a decrease in absorbance of the line at 912 cm<sup>-1</sup>, about 30% of propylene is oxidized during the plasma treatment. This observation of an incomplete oxidation of the hydrocarbon in the exhaust stream corresponds well with other published reports [7,14].

In Fig. 6, FTIR spectra are shown with and without plasma processing for the wave number region between 2000 and 650 cm<sup>-1</sup>. Without plasma, the band associated with NO can be seen near 1880 cm<sup>-1</sup> and three distinct bands associated with the presence of propylene are observed near 1655, 1440, and 920 cm<sup>-1</sup>. After plasma treatment, NO has been completely oxidized to NO<sub>2</sub>. The NO bands near 1880 cm<sup>-1</sup> are no longer present and features for the presence of NO<sub>2</sub> are observed at a wave number near 1620 cm<sup>-1</sup>. Oxidation of C<sub>3</sub>H<sub>6</sub> is also observed in this spectral region, with the presence of the sharp peaks associated with CO<sub>2</sub> and CH<sub>2</sub>O at 668 and 1748 cm<sup>-1</sup>, respectively. Also, the band associated with the stretch of the NO<sub>2</sub> group of a O–NO<sub>2</sub> group

of organic nitrates is observed at wave number near 1277 cm<sup>-1</sup>.

### 3.2. Heterogeneous catalytic activity

Extensive research is being done to use non-thermal plasma in combination with heterogeneous catalysis to remove NO<sub>x</sub> in lean burn exhaust [8,16–19]. In this study, two catalysts were investigated: sodium zeolite Y and  $\gamma$ -alumina. The NaY extrudates were provided by *Zeolyst International* and have a surface area of 800 m<sup>2</sup>/g and a SiO<sub>2</sub>:Al<sub>2</sub>O<sub>3</sub> ratio of 5. Gamma alumina is a metastable polycrystalline form of Al<sub>2</sub>O<sub>3</sub> that is commonly used as a catalyst or substrate due to its small particle size and high surface area. The surface area of the  $\gamma$ -alumina used in this study was 200 m<sup>2</sup>/g. Under exhaust condition temperatures below 900 °C,  $\gamma$ -alumina does not convert to its more stable phase  $\alpha$ -alumina.

### 3.3. Sodium zeolite Y

The percent NO<sub>x</sub> conversion as a function of catalyst temperature was measured for a two-stage system where the plasma was followed by a packed bed (20 ml) of NaY extrudates. The gas flow rate was 4 l/min and the space velocity was 12,000 h<sup>-1</sup>. As shown in Fig. 7, a maximum activity of 70% was achieved at 200 °C, and NO<sub>x</sub> efficiency decreased at higher and lower temperatures. FTIR analysis

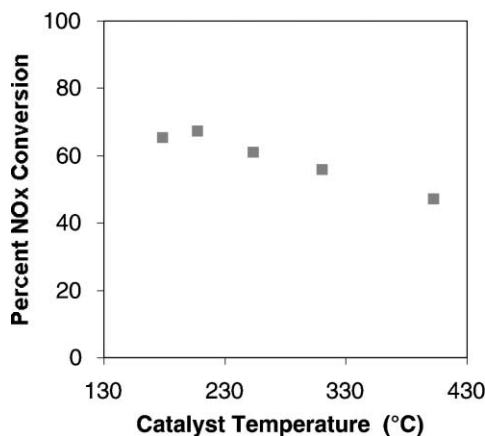


Fig. 7. The measured percent NO<sub>x</sub> conversion as a function of catalyst temperature for sodium zeolite Y.

Table 2

NO<sub>x</sub> and propylene conversion and concentrations of aldehydes during plasma and plasma-catalyst treatment

	NO <sub>x</sub> conversion (%)	C <sub>3</sub> H <sub>6</sub> conversion (%)	Formaldehyde (ppm)	Acetaldehyde (ppm)
Plasma <sup>a</sup>	12	20	85	95
Plasma-catalyst <sup>b</sup>	43	20	33	19

<sup>a</sup> 6% O<sub>2</sub>, 530 ppm C<sub>3</sub>H<sub>6</sub>, 200 ppm NO, 1% H<sub>2</sub>O.<sup>b</sup> 6% O<sub>2</sub>, 530 ppm C<sub>3</sub>H<sub>6</sub>, 200 ppm NO, 2% H<sub>2</sub>O.

detected aldehydes and N<sub>2</sub>O in the effluent gas leaving the catalyst at all temperatures. N<sub>2</sub>O concentrations were generally low (10–20 ppm). N<sub>2</sub>O concentrations decreased at higher catalyst temperatures. Aldehyde concentrations increased with the energy density and ranged from 150 to 250 ppm.

In separate experiments, the effect of plasma and plasma-catalyst treatments on hydrocarbon species in the stream was investigated. In these experiments both the plasma and catalyst temperature was 180 °C. The gas consisted of 200 ppm of NO, 6% O<sub>2</sub>, 600 ppm C<sub>3</sub>H<sub>6</sub>, and 1–2% H<sub>2</sub>O. The space velocity was 12,000 h<sup>-1</sup>. As we noticed earlier, H<sub>2</sub>O does not affect the chemistry in the plasma. Power deposited to the plasma was 30 J/l. Table 2 summarizes the experimental results. The lower overall conversion levels are due to the use of the less efficient plasma reactor configuration. As NO<sub>x</sub> is reduced over the catalyst bed, most of the aldehydes formed in the plasma are oxidized. At the same time, residual propylene passes over the catalyst without significant oxidation.

### 3.3.1. $\gamma$ -Al<sub>2</sub>O<sub>3</sub>

The percent NO<sub>x</sub> conversion as a function of catalyst temperature was also measured for a commercial  $\gamma$ -alumina. 10 ml of  $\gamma$ -alumina extrudates was used and the gas flow rate was 2 l/min (12,000 h<sup>-1</sup>). Fig. 8 shows the thermal (no plasma) activity of  $\gamma$ -alumina and the activity when the simulated lean NO<sub>x</sub> gases are plasma processed prior to contacting the  $\gamma$ -alumina. The  $\gamma$ -alumina showed some thermal activity with NO as the NO<sub>x</sub> input over the temperature range of 200–400 °C. The thermal activity increased with increasing temperature with a maximum conversion of 20% at 380 °C. Below 200 °C there was no thermal activity. With plasma, the activity is greatly enhanced. At temperatures above 250 °C, about 80% NO<sub>x</sub> conversion was observed.

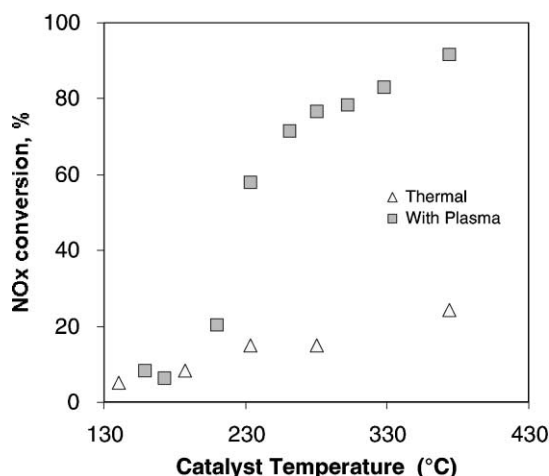


Fig. 8. The measured percent NO<sub>x</sub> conversion as a function of catalyst temperature for  $\gamma$ -alumina.

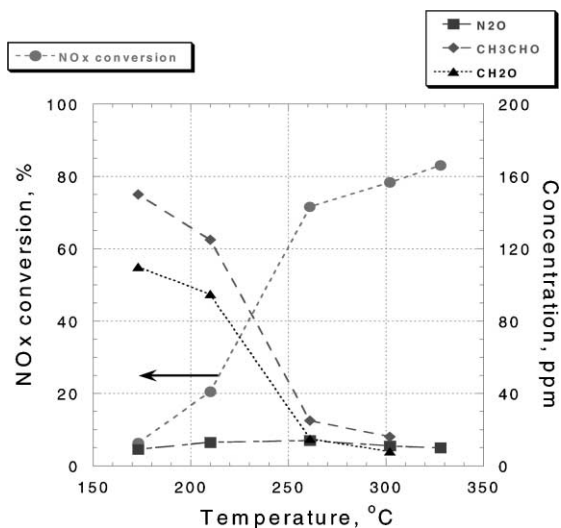


Fig. 9. The measured percent NO<sub>x</sub> conversion, concentrations of formaldehyde (CH<sub>2</sub>O), acetaldehyde (CH<sub>3</sub>CHO), and concentration of nitrous oxide (N<sub>2</sub>O) as a function of catalyst temperature for  $\gamma$ -alumina.

Acetaldehyde, formaldehyde, and  $\text{N}_2\text{O}$  concentrations were measured in the effluent gas leaving the  $\gamma$ -alumina. The concentrations of these species are plotted as a function of catalyst temperature and are compared to the  $\text{NO}_x$  conversion efficiency in Fig. 9. FTIR analysis shows an immediate drop in the aldehyde concentrations with a simultaneous increase in the percent  $\text{NO}_x$  conversion when the catalyst temperature was increased from 210 to 260 °C. This result indicates that aldehydes may participate in selective catalytic reduction of  $\text{NO}_x$  on this catalyst.  $\text{N}_2\text{O}$  concentrations were low over the entire temperature range.

#### 4. Conclusions

Plasma-assisted heterogeneous catalysis has been shown to be an effective process in the remediation of  $\text{NO}_x$  in synthetic lean burn gasoline and diesel CI exhaust. This study was undertaken to examine the role of plasma processing on lean  $\text{NO}_x$  reduction over NaY and  $\gamma$ -alumina.

The plasma-induced chemistry was measured with CLNA, and FTIR analysis and compared with published reports. The oxidation of the NO to  $\text{NO}_2$  in the presence of hydrocarbon by plasma processing was shown. Also, the incomplete oxidation of the hydrocarbon in the gas stream was shown through FTIR analysis.

The plasma-assisted heterogeneous catalytic activity of NaY and  $\gamma$ -alumina was presented as a function of temperature. It was shown that the NaY is most active in the temperature window of 180–230 °C and the activity decreases with increasing temperature. It was also shown that  $\gamma$ -alumina is most active at temperatures above 250 °C and relatively inactive at temperatures below 250 °C.

A simultaneous decrease in the  $\text{NO}_x$  and aldehyde concentrations was observed over both catalyst. This suggests that aldehydes formed during the plasma treatment of the simulated diesel exhaust may play an important role in subsequent  $\text{NO}_x$  reduction over the catalyst.

#### References

- [1] EPA environmental fact sheet, Office of Mobile Sources, EPA420-F-98-007, April 1998.
- [2] Plasma exhaust after treatment, SAE SP-1395, in: J. Hoard, H. Servati (Eds.), Society of Automotive Engineers, 1998.
- [3] Non-thermal plasma exhaust emission control, SAE SP-1483, in: M. Lou Balmer, G. Fisher, J. Hoard (Eds.), Society of Automotive Engineers, 1999.
- [4] Non-thermal plasma, SAE SP-1395, in: M. L. Balmer, G. Fisher, J. Hoard (Eds.), Society of Automotive Engineers, 1999.
- [5] M.L. Balmer, R.G. Tonkyn, A.Y. Kim, I.S. Yoon, D. Jimenez, T. Orlando, S. Barlow, J. Hoard, Diesel  $\text{NO}_x$  reduction on surfaces in plasma, SAE 982511, 1998.
- [6] G.E. Vogtlin, B.T. Merritt, M.C. Hsiao, P.H. Wallman, B.M. Penetrante, Plasma-assisted catalytic reduction system, US Patent 5,711,147, January 27 1998.
- [7] B.M. Penetrante, W.J. Pitz, M.C. Hsiao, B.T. Merritt, G.E. Vogtlin, Effect of hydrocarbons on plasma treatment of  $\text{NO}_x$ , in: Proceedings of the 1997 Diesel Engine Emissions Reduction Workshop.
- [8] B.M. Penetrante, R.M. Brusasco, B.T. Merritt, W.J. Pitz, G.E. Vogtlin, M.C. Kung, H.H. Kung, C.Z. Wan, K.E. Voss, Plasma-assisted catalytic reduction of  $\text{NO}_x$ , SAE 982508, 1998.
- [9] Non-thermal plasma techniques for pollution control. Part A: Overview, Fundamentals and Supporting Technologies, in: B.M. Penetrante, S.E. Schultheis (Eds.), Springer, Berlin, 1993.
- [10] L.A. Rosenthal, IEEE Trans. Ind. Appl. I-5, 338 (1973).
- [11] R.G. Tonkyn, S.E. Barlow, T.M. Orlando, J. Appl. Phys. 80 (9) (1996).
- [12] M.L. Balmer, R.G. Tonkyn, I.S. Yoon, S. Barlow, J. Hoard, Surface mediation of  $\text{NO}_x$  reduction/oxidation in a plasma, Mater. Soc. Symp. Proc. 549 (1999) 211–216.
- [13] R. Tonkyn, S. Barlow, M.L. Balmer, T. Orlando, J. Hoard, D. Goulette, Vehicle exhaust treatment using electrical discharge methods, SAE 971716, May 1997.
- [14] B.M. Penetrante, M.C. Hsiao, B.T. Merritt, G.E. Vogtlin, C.Z. Wan, G.W. Rice, K.E. Voss, Plasma-assisted heterogeneous catalysis for  $\text{NO}_x$  reduction in lean-burn engine exhaust, in: Proceedings of the 1997 Diesel Engine Emissions Reduction Workshop.
- [15] G.B. Fisher, C.L. DiMaggio, J.W. Sommers,  $\text{NO}_x$  Reactivity of prototype catalysts for a plasma-catalyst after treatment system, SAE 1999-01-3685.
- [16] M.L. Balmer, R.G. Tonkyn, A.Y. Kim, J. Hoard, I.S. Yoon, D. Jimenez, T. Orlando, S. Barlow, Nitrogen measurement from  $\text{NO}_x$  reduction for a plasma-catalyst system in simulated diesel exhaust, in: Proceedings of the 1998 Diesel Engine Emissions Reduction Workshop in Castine, Maine, 1998.
- [17] M.L. Balmer, R.G. Tonkyn, I.S. Yoon, A. Kolwaite, S. Barlow, G. Maupin, J. Hoard,  $\text{NO}_x$  destruction behavior of select materials when combined with a non-thermal plasma, SAE 1999-01-3640, October 1999.
- [18] J. Hoard, M.L. Balmer, Analysis of plasma-catalysis for diesel  $\text{NO}_x$  remediation, SAE 982429, 1998.
- [19] T. Oda, T. Kato, T. Takahashi, K. Shimizu, Nitric oxide decomposition in air by using nonthermal plasma processing with additives and catalyst, in: Proceedings of the IEEE Transactions on Industry Applications, Vol. 34, no. 2, 1998.